



Composition and light absorption of N-containing aromatic compounds in organic aerosols from laboratory biomass burning

Mingjie Xie^{1,2,3,4}, Xi Chen⁴, Michael D. Hays⁴, and Amara L. Holder⁴

¹Collaborative Innovation Center of Atmospheric Environment and Equipment Technology, Jiangsu Key Laboratory of Atmospheric Environment Monitoring and Pollution Control, School of Environmental Science and Engineering, Nanjing University of Information Science and Technology, 219 Ningliu Road, Nanjing 210044, China

²State Key Laboratory of Pollution Control and Resource Reuse, School of the Environment, Nanjing University, Nanjing, China

³Oak Ridge Institute for Science and Education (ORISE), Office of Research and Development, U.S. Environmental Protection Agency, 109 T.W. Alexander Drive, Research Triangle Park, NC 27711, USA

⁴National Risk Management Research Laboratory, Office of Research and Development, U.S. Environmental Protection Agency, 109 T.W. Alexander Drive, Research Triangle Park, NC 27711, USA

Correspondence: Mingjie Xie (mingjie.xie@colorado.edu, mingjie.xie@nuist.edu.cn)

Received: 7 October 2018 – Discussion started: 11 October 2018

Revised: 9 February 2019 – Accepted: 20 February 2019 – Published: 7 March 2019

Abstract. This study seeks to understand the compositional details of N-containing aromatic compounds (NACs) emitted during biomass burning (BB) and their contribution to light-absorbing organic carbon (OC), also termed brown carbon (BrC). Three laboratory BB experiments were conducted with two United States pine forest understory fuels typical of those consumed during prescribed fires. During the experiments, submicron aerosol particles were collected on filter media and subsequently extracted with methanol and examined for their optical and chemical properties. Significant correlations ($p < 0.05$) were observed between BrC absorption and elemental carbon (EC)/OC ratios for individual burns data. However, the pooled experimental data indicated that EC/OC alone cannot explain the BB BrC absorption. Fourteen NAC formulas were identified in the BB samples, most of which were also observed in simulated secondary organic aerosol (SOA) from photooxidation of aromatic volatile organic compounds (VOCs) with NO_x . However, the molecular structures associated with the identical NAC formula from BB and SOA are different. In this work, the identified NACs from BB are featured by methoxy and cyanate groups and are predominately generated during the flaming phase. The mass concentrations of identified NACs were quantified using authentic and surrogate standards, and their contributions to bulk light absorption of

solvent-extractable OC were also calculated. The contributions of identified NACs to organic matter (OM) and BrC absorption were significantly higher in flaming-phase samples than those in smoldering-phase samples, and they correlated with the EC/OC ratio ($p < 0.05$) for both individual burns and pooled experimental data, indicating that the formation of NACs from BB largely depends on burn conditions. The average contributions of identified NACs to overall BrC absorption at 365 nm ranged from $0.087 \pm 0.024 \%$ to $1.22 \pm 0.54 \%$, which is 3–10 times higher than their mass contributions to OM ($0.023 \pm 0.0089 \%$ to $0.18 \pm 0.067 \%$), so the NACs with light absorption identified in this work from BB are likely strong BrC chromophores. Further studies are warranted to identify more light-absorbing compounds to explain the unknown fraction ($> 98 \%$) of BB BrC absorption.

1 Introduction

Biomass burning (BB), including residential burning for cooking, heating, and open burning, is a major source of atmospheric carbonaceous aerosol, contributing 62 % and 93 % of black carbon (BC) and primary organic carbon (OC) particle emissions, respectively (Bond et al., 2004). BC can absorb sunlight across the entire spectral range with a weak

dependence on wavelength (λ) (Bond, 2001; Bond et al., 2013; Lack and Langridge, 2013). OC in particulate matter (PM) is commonly treated as a purely light-scattering component in global climate models (Chung and Seinfeld, 2002; Myhre et al., 2013). Recent field and laboratory studies found that the light absorption of BB OC increases rapidly from the purple-green region (400–550 nm) to the near-ultraviolet (UV) region (300–400 nm) (Kirchstetter et al., 2004; Laskin et al., 2015; Chakrabarty et al., 2016; Xie et al., 2017b). The light absorption and scattering by BC and OC from BB can directly affect the Earth's radiative balance (Ramanathan et al., 2001; Anderson et al., 2003; Bond and Bergstrom, 2006), and BC emission factors and their warming effect have been intensively investigated (Bond et al., 2004, 2013). However, the optical properties and chemical composition of light-absorbing OC, also termed brown carbon (BrC), from BB are less well characterized. The chromophores in BrC are expected to have a high degree of unsaturation or conjugation (Chen and Bond, 2010; Lin et al., 2014; Laskin et al., 2015) but are seldom identified and used as BrC tracers in the atmosphere (Desyaterik et al., 2013; Zhang et al., 2013; Teich et al., 2016).

Polycyclic aromatic hydrocarbons (PAHs) and their derivatives are typical BrC chromophores (Samburova et al., 2016; Huang et al., 2018), of which the light absorption in the UV and visible wavelength range is highly dependent on ring numbers and the degree of conjugation (Samburova et al., 2016). However, PAH emissions are not source-specific but are associated with multiple different combustion processes, including BB (Samburova et al., 2016), coal burning (Chen et al., 2005), and motor vehicle emissions (Riddle et al., 2007). Therefore, PAHs are not unique to BB BrC. N-containing aromatic compounds (NACs) are another class of BrC chromophores that have been detected in BB (Lin et al., 2016), cloud water (Desyaterik et al., 2013) and atmospheric particles (Zhang et al., 2013; Teich et al., 2017). In water extracts of atmospheric particles, NACs can contribute more than 3 % of the light absorption at 365–370 nm (Zhang et al., 2013; Teich et al., 2017). These results suggest that NACs are important BrC chromophores, but their composition and structures are less certain for BB aerosols. Nitrophenols, nitrocatechols, and methyl nitrocatechols (including isomers) are commonly observed in BB aerosols (Iinuma et al., 2010; Claeys et al., 2012; Lin et al., 2016, 2017) and are also generated from the photooxidation of benzene, toluene, and *m*-cresol in the presence of NO_x (Iinuma et al., 2010; Lin et al., 2015; Xie et al., 2017a). As such, other NAC structures specific to BB are needed to represent BB BrC chromophores. Additionally, very few studies have examined the influence of burn conditions on the formation of NACs in BB emissions, although it is well known that increasing combustion temperature, or flaming-dominated combustion, is associated with strong BrC absorption (Chen and Bond, 2010; Saleh et al., 2014).

The present study attempts to characterize the compositional profile of NACs from BB, identify additional NAC structures in laboratory BB samples, and evaluate the contributions of NACs to bulk absorption of solvent-extractable OC from BB. A high-performance liquid chromatograph interfaced to a diode array detector (HPLC/DAD) and quadrupole (Q) time-of-flight mass spectrometer (ToF-MS) was used to examine NACs in $\text{PM}_{2.5}$ (particulate matter with aerodynamic diameter $\leq 2.5 \mu\text{m}$) from three BB experiments. A thermal-optical instrument determined bulk OC and elemental carbon (EC) in the PM, and a UV-visible (UV-Vis) spectrometer was used to measure total BrC absorption in methanol extracts of BB $\text{PM}_{2.5}$. In this work, a number of NAC formulas with structures that might be specifically related to BB were identified, and the contributions of identified NACs to bulk BrC absorption were calculated. These results shed light on the light-absorbing characteristics of BB OC at bulk chemical and molecular levels, benefiting the understanding of BrC sources and chromophores.

2 Methods

2.1 Laboratory open BB simulations

Laboratory simulations of open BB were conducted at the U.S. EPA (Research Triangle Park, RTP; North Carolina, NC) Open Burn Test Facility (OBTF), a 70 m^3 enclosure, as detailed in Grandesso et al. (2011). Details of the protocols for biomass fuel collection and burn simulations were provided elsewhere (Aurell and Gullett, 2013; Aurell et al., 2015; Holder et al., 2016). Briefly, forest understory fuels were gathered from two different locations in the southeastern United States – Florida (FL) and NC. The FL forest field (Eglin Air Force Base, FL) is characteristic of a well-managed long leaf pine (*Pinus palustris*) ecosystem. The NC forest was located near the EPA campus in RTP, and it contained mainly loblolly pine (*Pinus taeda*) with some deciduous hardwood tree leaf litter. Biomass fuel was divided by a quartering procedure (Aurell and Gullett, 2013) and burned in batches (1 kg) on an aluminum-foil-coated steel pan (1 m \times 1 m). Ambient air was pulled into the OBTF through a large inlet at ground level and the combustion exhaust was drawn through a roof duct near a baghouse using a high-volume blower. $\text{PM}_{2.5}$ was sampled at 10 L min^{-1} on Teflon (47 mm, Pall, Ann Arbor, Michigan, USA) and preheated (550 °C, 12 h) quartz filters (QF, diameter 43 mm, Pall) with a $\text{PM}_{2.5}$ impactor (SKC, Pittsburgh, Pennsylvania, USA). For the NC forest fire simulation, filter samples were collected during an initial flaming phase lasting approximately 1–3 min. After most of the flames were extinguished, a second set of filter samples were obtained for the smoldering emissions. Smoldering samples were collected until there was little or no visible smoke being emitted from the fuel bed, typically lasting 6–15 min. Two separate experiments

were done with the NC forest fuels in spring and summer, respectively, with different ambient temperatures (Table S1 in the Supplement). Sampling of the FL forest fire simulations was done in fall over the complete burn and was not divided into flaming and smoldering phases. Only one experiment was done for the FL forest fuels collected in fall. Background samples were obtained post-burn inside the OBTF. A summary of the sample information is provided in Table S1.

2.2 Bulk carbon and light absorption measurement

Details of the bulk OC, EC, and light absorption analysis methods are provided in Xie et al. (2017a, b). Briefly, the bulk OC and EC were measured using an OC–EC analyzer (Sunset Laboratories, Portland, OR) with a modified NIOSH method 5040 protocol (NIOSH, 1999). For light absorption measurement, one filter punch (1.5 cm²) was extracted in 5 mL methanol (HPLC grade) ultrasonically for 15 min and then filtered through a 30 mm diameter polytetrafluoroethylene (PTFE) filter with a 0.2 μm pore size (National Scientific Company). The light absorption of methanol extracts was measured with a UV–Vis spectrometer (V660, Jasco Incorporated, Easton MD) over the wavelength range of 200 to 900 nm. To ensure data quality, the wavelength accuracy (±0.3 nm) and repeatability (±0.05 nm) were tracked every month with a NIST traceable holmium oxide standard. Solvent background was subtracted with a reference cuvette containing pure methanol. The extracted filter was air-dried in a fume hood overnight, and the residual OC was measured with the Sunset thermal–optical analyzer. The extraction efficiency (η, %) of OC by methanol is calculated by

$$\eta = \frac{OC_b - OC_r}{OC_b} \times 100\%, \quad (1)$$

where OC_b is the OC content of the PM_{2.5} filter before extraction and OC_r is the OC content in the air-dried filter after extraction.

The light absorption coefficient of the methanol extracts (Abs_λ, Mm⁻¹) is calculated as

$$Abs_\lambda = (A_\lambda - A_{700}) \times \frac{V_l}{V_a \times L} \ln(10), \quad (2)$$

where A₇₀₀ is subtracted from A_λ to correct baseline drift, V_l (m³) is the solvent volume (5 mL) used for extraction, V_a (m³) is the air volume of the extracted filter area, L (0.01 m) is the optical path length, and ln(10) converts the absorption coefficient in units of m⁻¹ from log base 10 to natural log (Hecobian et al., 2010). The bulk mass absorption coefficient (MAC_λ, m² g C⁻¹) is calculated by

$$MAC_\lambda = \frac{Abs_\lambda}{C_{OC}}, \quad (3)$$

where C_{OC} is the mass concentration of extractable OC (OC_b – OC_r) for each filter sample (μg m⁻³). The solution

absorption Ångström exponent (Å_{abs}) is determined from the slope of the linear regression of log₁₀(Abs_λ) vs. log₁₀(λ) over the λ range of 300 to 550 nm. In the current work, Abs_λ and MAC_λ were focused at 365 and 550 nm, representing the BrC absorption at the near-UV and visible regions, respectively (Zhang et al., 2013; Saleh et al., 2014). The EC/OC ratio, methanol extraction efficiency (η), and light-absorbing properties (Abs_λ, MAC_λ, and Å_{abs}) of each BB sample are listed in Table S1 in the Supplement and summarized in Table 1.

2.3 Filter extraction and HPLC/DAD-Q-ToF-MS analysis

The PM_{2.5} filter extraction and subsequent instrumental analysis methods used here are the same as those described in Xie et al. (2017a). Briefly, a 4–6 cm² piece of each filter was pre-spiked with 25 μL of 10 ng μL⁻¹ nitrophenol-d4 (internal standard, IS) and extracted ultrasonically in 3–5 mL of methanol twice (15 min each). After filtration and concentration, the final volume was roughly 500 μL prior to HPLC/DAD-Q-ToF-MS analysis. An Agilent 1200 series HPLC equipped with a Zorbax Eclipse Plus C18 column (2.1 mm × 100 mm, 1.8 μm particle size, Agilent Technologies) was used to separate the target NACs with an injection volume of 2 μL. The flow rate of the column was set at 0.2 mL min⁻¹, and the gradient separation was conducted with 0.2 % acetic acid (v/v) in water (eluent A) and methanol (eluent B). The concentration of eluent B was 25 % for the first 3 min, increased to 100 % from 3 to 10 min, held at 100 % from 10 to 32 min, and then decreased back to 25 % from 32 to 37 min. The identification and quantification of NACs were determined with an Agilent 6520 Q-ToF-MS. The Q-ToF-MS was equipped with a multimode ion source operating in electrospray ionization (ESI) and negative (–) ion modes. All samples were analyzed in full scan mode (40–1000 Da), and an acceptance criterion of ±10 ppm mass accuracy was set for compound identification and quantification. Then selected samples were re-examined using the collision-induced dissociation (CID) technique under identical chromatographic conditions. The MS/MS spectra of target [M–H][–] ions provided m/z data, which were used for identifying NAC structures.

The extracted ion chromatograms (EICs) and Q-ToF MS/MS spectra for identified compounds in selected BB samples are provided in Fig. S1 in the Supplement and in Fig. 1, respectively. The Q-ToF MS/MS spectra of standard and surrogate compounds used in this work are obtained from Xie et al. (2017a) and provided in Fig. S2 for comparison. Table 2 provides the formulas, standard and surrogate assignments, and proposed structures of the identified NACs. Due to the lack of authentic standards, most of the NACs in BB samples were quantified using surrogates in this work. In general, the surrogate compound with similar molecular weight (MW) and/or structure was selected for the mass quantification of each identified NAC. Since the

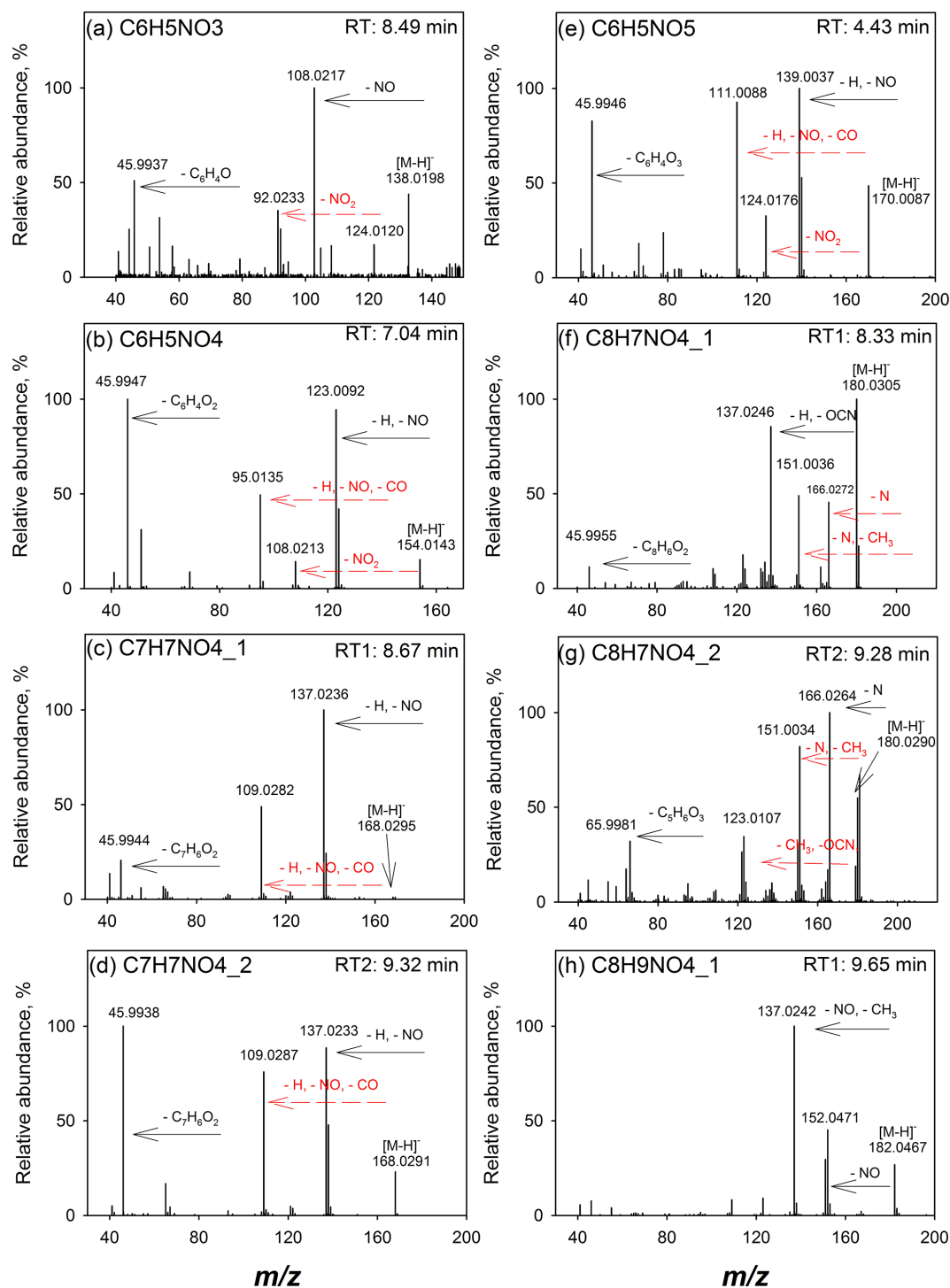


Figure 1.

standard compound with hydroxyphenyl cyanate structure is not commercially available, C₈H₇NO₄ and C₉H₉NO₄ were quantified as 2-methyl-5-nitrobenzoic acid (C₈H₇NO₄) and 2,5-dimethyl-4-nitrobenzoic acid (C₉H₉NO₄), respectively; all the identified NACs with MW > 200 Da were quantified as 2-nitrophenol (C₆H₅NO₂). The mass quantifica-

tion was conducted using the internal standard method with nine-point calibration curves ($\sim 0.01\text{--}2\text{ ng }\mu\text{L}^{-1}$). The compounds corresponding to each NAC formula (including isomers) were quantified individually and added together for the calculation of mass contribution (%) to organic matter (OM $\mu\text{g m}^{-3}$) in each sample. The quality assurance and con-

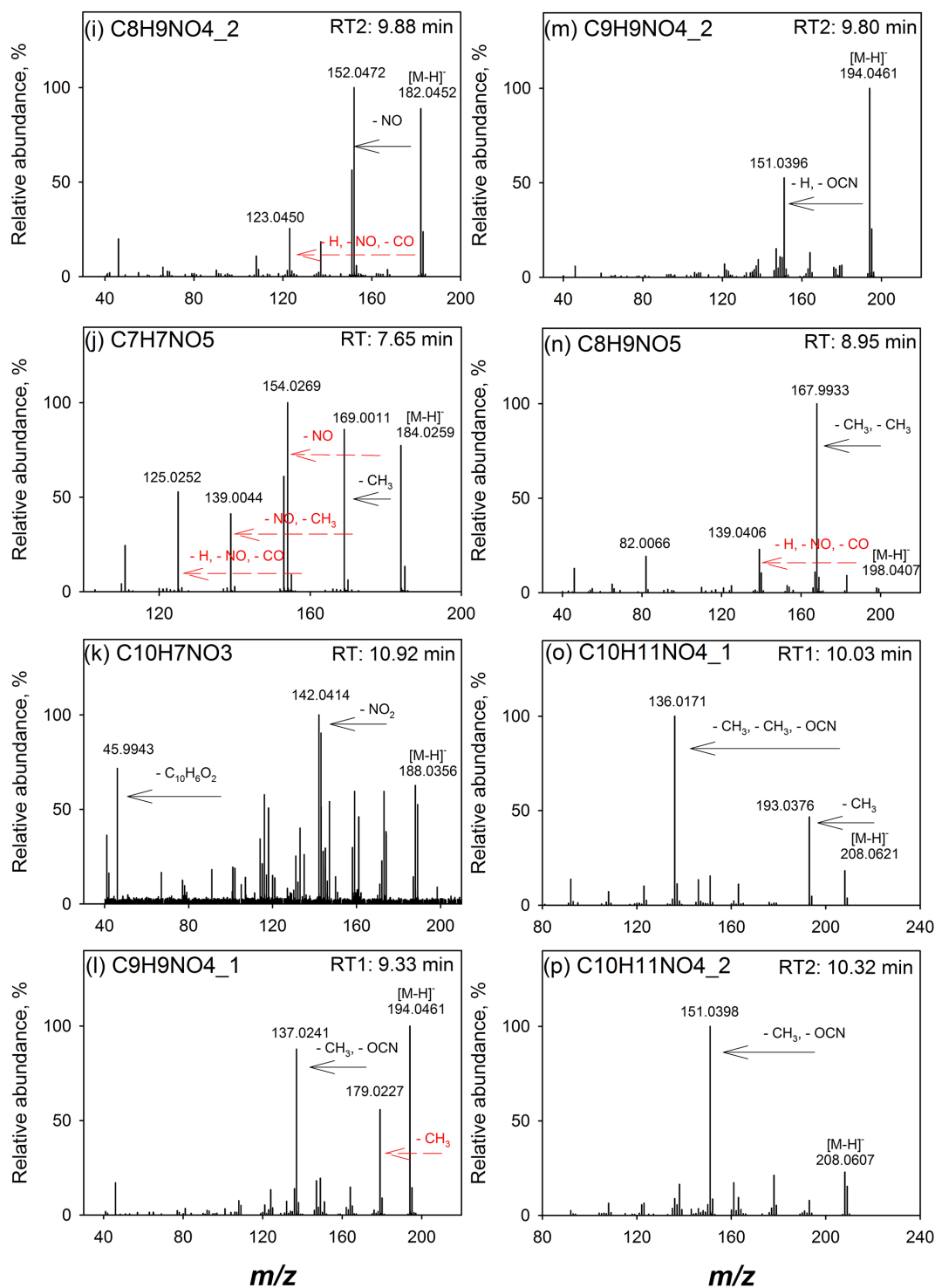


Figure 1.

trol (QA/QC) procedures applied for NAC quantification were provided in Xie et al. (2017a). Field blank and background samples were free of contamination for NACs. Average recoveries of standard compounds ranged from 75.1 %

to 116 %, and the method detection limit ranged from 0.70 to 17.6 pg (Table S2).

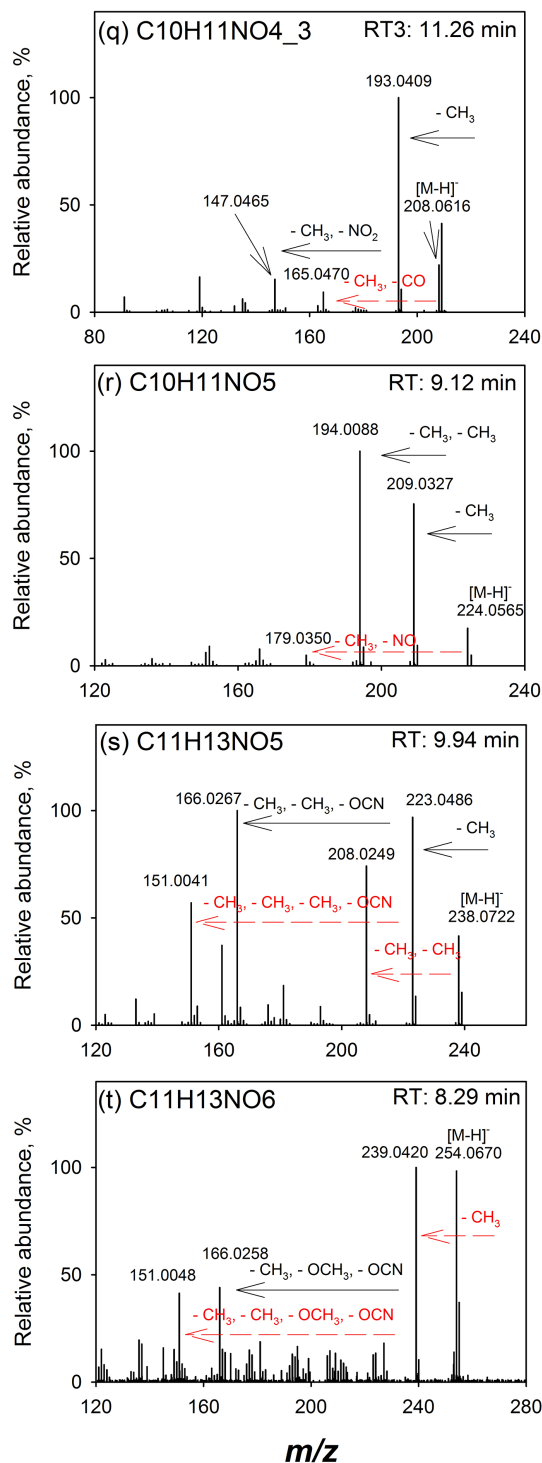


Figure 1. Q-ToF MS/MS spectra of (a) $C_6H_5NO_3$, (b) $C_6H_5NO_4$, (c, d) $C_7H_7NO_4$ isomers, (e) $C_6H_5NO_5$, (f, g) $C_8H_7NO_4$ isomers, (h, i) $C_8H_9NO_4$ isomers, (j) $C_7H_7NO_5$, (k) $C_{10}H_7NO_3$, (l, m) $C_9H_9NO_4$ isomers, (n) $C_8H_9NO_5$, (o–q) $C_{10}H_{11}NO_4$ isomers, (r) $C_{10}H_{11}NO_5$, (s) $C_{11}H_{13}NO_5$, and (t) $C_{11}H_{13}NO_6$ identified in the flaming-phase sample collected during the NC forest 1 experiment, burn 2 (Table S1).

3 Results and discussion

3.1 Light absorption of extractable OC

The average EC/OC ratio, OC extraction efficiency, MAC_{365} , MAC_{550} , and \hat{A}_{abs} of all samples grouped by experiment and fire phase are shown in Table 1. Abbreviations for each sample group are also listed in the table. The optical properties and bulk composition of the FL forest samples were reported in Xie et al. (2017b). The average extraction efficiency for all groups of BB samples is greater than 95 % (range 97.0 ± 1.87 % to 99.5 ± 0.33 %), and the light absorption exhibits strong wavelength dependence, with average \hat{A}_{abs} values ranging from 5.68 ± 0.70 to 7.95 ± 0.22 . For each of the two NC forest experiments, the samples collected during the flaming phase (NF1 and NF2) have significantly higher (Student's *t* test, $p < 0.05$) average EC/OC ratios, MAC_{365} , and MAC_{550} and lower ($p < 0.05$) \hat{A}_{abs} than those collected during the smoldering phase (NS1 and NS2). When combining the results from the two NC forest experiments, the average MAC_{365} values for NC forest 2 are significantly ($p < 0.05$) higher than NC forest 1, despite having a comparable EC/OC ratio (NF1 = 0.042 ± 0.014 and NF2 = 0.049 ± 0.011 , NS1 = 0.0098 ± 0.0024 and NS2 = 0.0075 ± 0.0026). Additionally, the average EC/OC ratio of FF samples is 5–30 times higher than the NF and NS samples, while the average MAC_{365} and MAC_{550} values of FF samples (1.13 ± 0.15 and 0.053 ± 0.023 $m^2 g C^{-1}$) are comparable to NS1 samples (1.10 ± 0.11 and 0.054 ± 0.015 $m^2 g C^{-1}$) but lower than other NC forest samples.

High-temperature pyrolysis or intense flaming conditions are known to increase the fraction of EC in the total carbonaceous aerosol emissions of BB (Hosseini et al., 2013; Eriksson et al., 2014; Martinsson et al., 2015; Nielsen et al., 2017). Several studies found that the light-absorbing properties of BB OC could be parameterized as a function of the EC/OC or BC/OA (organic aerosol) ratio, a measurement proxy for burn conditions (McMeeking et al., 2014; Saleh et al., 2014; Lu et al., 2015; Pokhrel et al., 2016), and inferred that the absorptivity of BB OC depended strongly on burn conditions, not fuel type. In Xie et al. (2017b), significant correlations ($p < 0.05$) between MAC_{365} of methanol-extractable OC from BB and EC/OC ratios were observed only for samples with identical fuel type but not for pooled samples with different fuel types, indicating that both burn conditions and fuel types can impact the light absorption of BB OC. The contradiction is possibly ascribed to different approaches used in characterizing the light absorption of BB OC and different test fuel types (Xie et al., 2017b). In the current work, we combined the sample measurements from all three BB experiments and analyzed the correlations of bulk MAC_{365} vs. EC/OC. For the analysis, we removed one FL forest experiment sample due to the extremely high EC/OC ratio of 0.58 (burn 3, Table S1). Generally, EC/OC ratios are < 0.4 for laboratory BB (Akagi et al., 2011; Pokhrel et

Table 1. EC/OC ratio, OC extraction efficiency, and light-absorbing properties of organic aerosols in PM_{2.5} from laboratory biomass burning.

Experiment	Phase	Abbr.	Fuels	EC/OC	Extraction efficiency (%)	MAC ₃₆₅ (m ² g C ⁻¹)	MAC ₅₅₀ (m ² g C ⁻¹)	Å _{abs}
FL forest ^a	No separation	FF	long leaf pine (<i>N</i> = 9)	0.21 ± 0.16	97.0 ± 1.87	1.13 ± 0.15	0.053 ± 0.023	7.36 ± 0.59
NC forest 1	Flaming	NF1	hardwood and loblolly pine (<i>N</i> = 3)	0.042 ± 0.014	97.7 ± 0.41	1.47 ± 0.25	0.15 ± 0.065	5.68 ± 0.70
	Smoldering	NS1	hardwood and loblolly pine (<i>N</i> = 3)	0.0098 ± 0.0024	97.9 ± 0.22	1.00 ± 0.11	0.054 ± 0.015	6.83 ± 0.52
NC forest 2	Flaming	NF2	hardwood and loblolly pine (4)	0.049 ± 0.011	99.5 ± 0.33	4.07 ± 0.15	0.17 ± 0.0051	7.38 ± 0.069
	Smoldering	NS2	hardwood and loblolly pine (4)	0.0075 ± 0.0026	99.2 ± 0.10	3.25 ± 0.35	0.12 ± 0.033	7.95 ± 0.22

^a Data were obtained from Xie et al. (2017b).

al., 2016; Xie et al., 2017b) and ≤ 0.1 for field BB (Au-rell et al., 2015; Xie et al., 2017b; Zhou et al., 2017). Thus, the burn condition of the FL forest burn 3 (Table S1) is unrepresentative of laboratory BB simulations or field BB. In Fig. 2a, the bulk MAC₃₆₅ of methanol-extracted OC correlated significantly ($p < 0.05$) with EC/OC for each BB experiment. However, grouping these sample measurements resulted in no correlation between MAC₃₆₅ and the EC/OC ratio (Fig. 2b). Similar results were also observed for MAC₅₅₀ vs. EC/OC and Å_{abs} vs. EC/OC correlations (Fig. S3a–d). These results show that BB BrC absorption depends on more than fire conditions, and light-absorbing components can be formed at relatively low EC/OC (e.g., tar balls) from smoldering biomass combustion (Chakrabarty et al., 2010).

In this work, both the comparison of the flaming versus smoldering samples for each NC experiment (Table 1) and the regressions of bulk MAC₃₆₅ versus EC/OC for individual burns (Fig. 2a) suggest that the light absorption of OC from BB is strongly dependent on burn conditions when the fuel type and ambient conditions are similar. The comparison of the FL versus NC forest experiments (Table 1) and the relationship between bulk MAC₃₆₅ and EC/OC for grouped measurements (Fig. 2b) indicate that the burn conditions are not the only factor impacting BB OC absorption. The two NC forest experiments were conducted in spring and summer, respectively, with distinct ambient conditions (Table S1), and their average MAC₃₆₅ values were significantly ($p < 0.05$) different. This could be partly ascribed to the fact that more semi-volatile organic compounds (SVOCs) will partition into the gas phase in summer with higher ambient temperatures, and the SVOC is less light-absorbing than OC with low volatility (Chen and Bond, 2010; Saleh et al., 2014). However, if the relative abundance of EC and OC from BB emissions is similar between the two NC forest experiments, the evaporation of SVOCs in summer will lead to higher EC/OC ratios, which is not observed in Table 1. No previous study investigated the seasonal variation in BrC absorption from

BB with similar fuel type. Chen et al. (2001) found that the ambient temperature might play a role in EC production from traffic by changing the air density. We suspected that the BB samples from NC forest 2 combustion in summer contained much stronger light-absorbing components than those from NC forest 1 combustion in spring, although the formation mechanism of these strong BrC components is uncertain and merits further study. Therefore, the light absorption of BB OC is influenced by factors other than burn conditions, and EC/OC ratios alone may not predict BB OC light absorption from burns with varying fuel types and ambient conditions.

3.2 Identification and quantification of NACs

In the current work, 14 NAC chemical formulas in BB samples were identified (Table 2) using the HPLC/DAD-Q-ToF-MS analysis, covering all the NACs with high abundance and strong absorption in ambient and BB particles reported in previous work (Claeys et al., 2012; Mohr et al., 2013; Zhang et al., 2013; Chow et al., 2016; Lin et al., 2016, 2017). Their EICs are provided in Fig. S1. The NAC structures corresponding to each chemical formula were examined using MS/MS data in Fig. 1. In Table S3, the averages and ranges of relative mass contributions of identified NACs to OM are provided by the BB experiment and burn condition. Here the OM mass was calculated as $1.7 \times \text{OC mass}$ (Reff et al., 2009). In addition, the average relative mass contributions of each NAC in BB samples are shown in Fig. 3.

The three BB experiments have consistent mass contribution profiles (Fig. 3), although they used different fuel types and were conducted in different seasons. In Table S3, the BB samples collected during flaming periods (NF1 and NF2) contain significantly higher ($p < 0.05$) average relative mass contributions from total NACs to OM (tNAC_{OM} %: NF1 $0.18 \pm 0.067\%$, NF2 $0.16 \pm 0.045\%$) than those collected during smoldering periods (NS1 $0.055 \pm 0.026\%$, NS2 $0.023 \pm 0.0089\%$). During the FL forest burn experiment,

Table 2. Identified N-containing aromatic compounds by HPLC/ESI-Q-ToF-MS from laboratory biomass burning in this study.

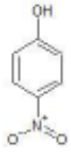
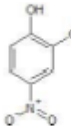
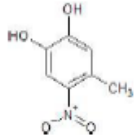
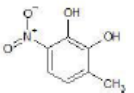
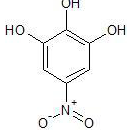
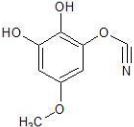
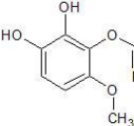
Suggested formula	Theoretical m/z [M-H] ⁻	Measured m/z [M-H] ⁻	Proposed structure	Quantified as ^b	Absorbing as ^c
C ₆ H ₅ NO ₃	138.0196	138.0198		4-Nitrophenol (C ₆ H ₅ NO ₃)	4-Nitrophenol (C ₆ H ₅ NO ₃)
C ₆ H ₅ NO ₄	154.0145	154.0143		4-Nitrocatechol (C ₆ H ₅ NO ₄)	4-Nitrocatechol (C ₆ H ₅ NO ₄)
C ₇ H ₇ NO ₄ (Iso1 ^a)	168.0302	168.0295		2-Methyl-4-nitroresorcinol (C ₇ H ₇ NO ₄)	2-Methyl-4-nitroresorcinol (C ₇ H ₇ NO ₄)
C ₇ H ₇ NO ₄ (Iso2)	168.0302	168.0291		2-Methyl-4-nitroresorcinol (C ₇ H ₇ NO ₄)	2-Methyl-4-nitroresorcinol (C ₇ H ₇ NO ₄)
C ₆ H ₅ NO ₅	170.0095	170.0087		2-Nitrophenol (C ₆ H ₅ NO ₅)	2-Nitrophenol (C ₆ H ₅ NO ₅)
C ₈ H ₇ NO ₄ (Iso1)	180.0302	180.0305		2-Methyl-5-nitrobenzoic acid (C ₈ H ₇ NO ₄)	Phenyl cyanate (C ₇ H ₅ NO)
C ₈ H ₇ NO ₄ (Iso2)	180.0302	180.0290		2-Methyl-5-nitrobenzoic acid (C ₈ H ₇ NO ₄)	Phenyl cyanate (C ₇ H ₅ NO)

Table 2. Continued.

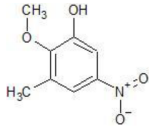
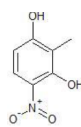
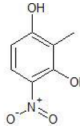
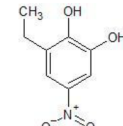
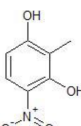
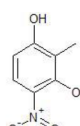
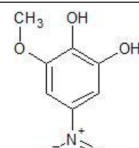
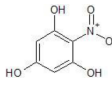
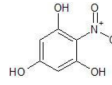
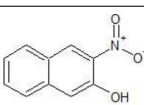
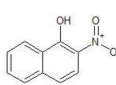
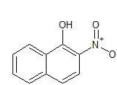
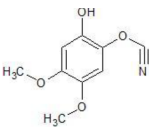
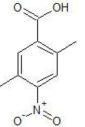
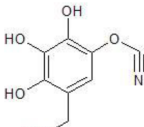
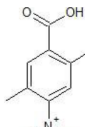
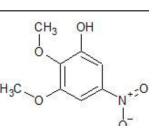
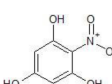
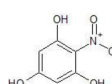
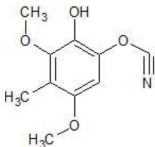
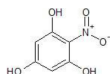
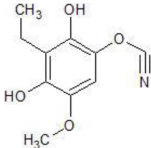
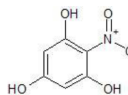
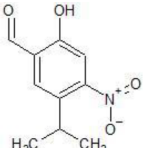
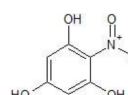
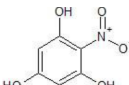
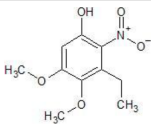
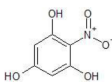
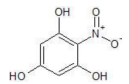
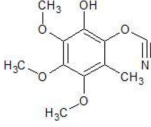
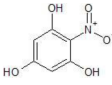
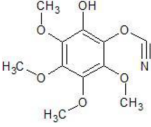
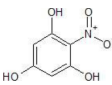
Suggested formula	Theoretical m/z [M-H] ⁻	Measured m/z [M-H] ⁻	Proposed structure	Quantified as ^b	Absorbing as ^c
C ₈ H ₉ NO ₄ (Iso1)	182.0459	182.0467		 2-Methyl-4-nitroresorcinol (C ₇ H ₇ NO ₄)	 2-Methyl-4-nitroresorcinol (C ₇ H ₇ NO ₄)
C ₈ H ₉ NO ₄ (Iso2)	182.0459	182.0452		 2-Methyl-4-nitroresorcinol (C ₇ H ₇ NO ₄)	 2-Methyl-4-nitroresorcinol (C ₇ H ₇ NO ₄)
C ₇ H ₇ NO ₅	184.0253	184.0259		 2-Nitrophenol (C ₆ H ₅ NO ₅)	 2-Nitrophenol (C ₆ H ₅ NO ₅)
C ₁₀ H ₇ NO ₃	188.0353	188.0356		 2-Nitro-1-naphthol (C ₁₀ H ₇ NO ₃)	 2-Nitro-1-naphthol (C ₁₀ H ₇ NO ₃)
C ₉ H ₉ NO ₄ (Iso1)	194.0458	194.0461		 2,5-Dimethyl-4-nitrobenzoic acid (C ₉ H ₉ NO ₄)	 Phenyl cyanate (C ₇ H ₅ NO)
C ₉ H ₉ NO ₄ (Iso2)	194.0458	194.0461		 2,5-Dimethyl-4-nitrobenzoic acid (C ₉ H ₉ NO ₄)	 Phenyl cyanate (C ₇ H ₅ NO)
C ₈ H ₉ NO ₅	198.0407	198.0407		 2-Nitrophenol (C ₆ H ₅ NO ₅)	 2-Nitrophenol (C ₆ H ₅ NO ₅)

Table 2. Continued.

Suggested formula	Theoretical m/z [M-H] ⁻	Measured m/z [M-H] ⁻	Proposed structure	Quantified as ^b	Absorbing as ^c
C ₁₀ H ₁₁ NO ₄ (Iso1)	208.0615	208.0621		 2-Nitrophenol (C ₆ H ₅ NO ₂)	 Phenyl cyanate (C ₇ H ₅ NO)
C ₁₀ H ₁₁ NO ₄ (Iso2)	208.0615	208.0607		 2-Nitrophenol (C ₆ H ₅ NO ₂)	 Phenyl cyanate (C ₇ H ₅ NO)
C ₁₀ H ₁₁ NO ₄ (Iso3)	208.0615	208.0616		 2-Nitrophenol (C ₆ H ₅ NO ₂)	 2-Nitrophenol (C ₆ H ₅ NO ₂)
C ₁₀ H ₁₁ NO ₅	224.0564	224.0565		 2-Nitrophenol (C ₆ H ₅ NO ₂)	 2-Nitrophenol (C ₆ H ₅ NO ₂)
C ₁₁ H ₁₃ NO ₅	238.0721	238.0722		 2-Nitrophenol (C ₆ H ₅ NO ₂)	 Phenyl cyanate (C ₇ H ₅ NO)
C ₁₁ H ₁₃ NO ₆	254.0670	254.0670		 2-Nitrophenol (C ₆ H ₅ NO ₂)	 Phenyl cyanate (C ₇ H ₅ NO)

^a Isomer 1; ^b standard compounds used for the quantification of identified N-containing aromatic compounds; ^c standard compounds used to estimate the light absorption of N-containing aromatic compounds.

flaming and smoldering phases were not separated for sampling, and the average tNAC_{OM} % is 0.13 ± 0.059 %, which is between the tNAC_{OM} % of the flaming and smoldering samples of the NC forest experiments. If we recalculate the average tNAC_{OM} % for the NC forest experiments by combining the flaming and smoldering sample data in

each burn, the three BB experiments (FL forest, NC forest 1, and NC forest 2) show similar average tNAC_{OM} % (0.11 ± 0.017 %–0.13 ± 0.059 %), and the average tNAC_{OM} % across all samples in this work is 0.12 ± 0.051 % (range 0.037 % to 0.21 %). This value is comparable to that observed at Detling (~ 0.5 %), United Kingdom, during win-

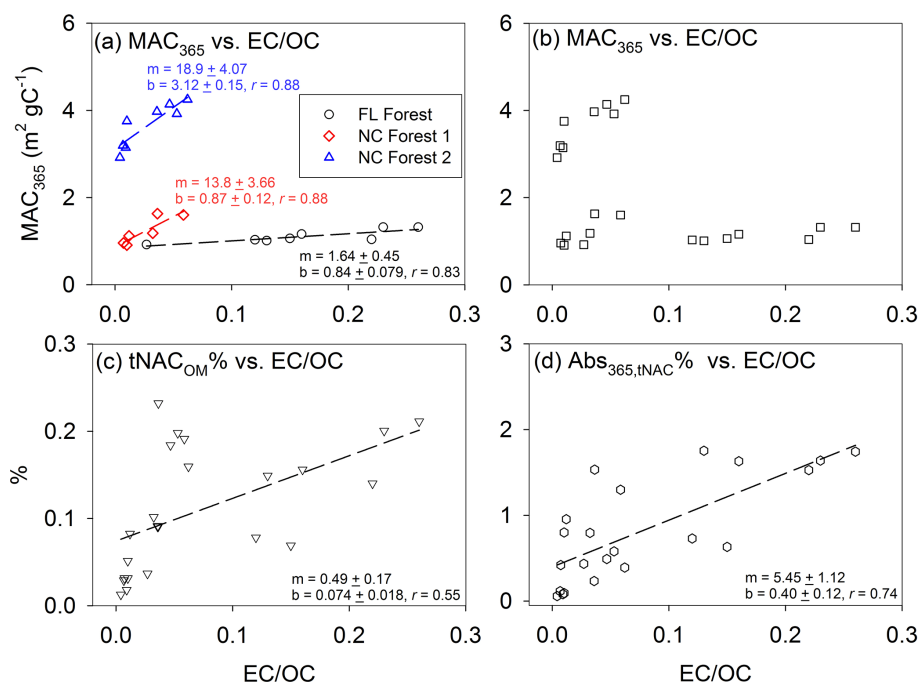


Figure 2. Linear regressions of (a) MAC₃₆₅ vs. EC/OC with individual burns data, (b) MAC₃₆₅ vs. EC/OC, (c) tNAC_{OM} % vs. EC/OC, and (d) Abs_{365,tNAC} % vs. EC/OC with pooled measurements of all the three experiments.

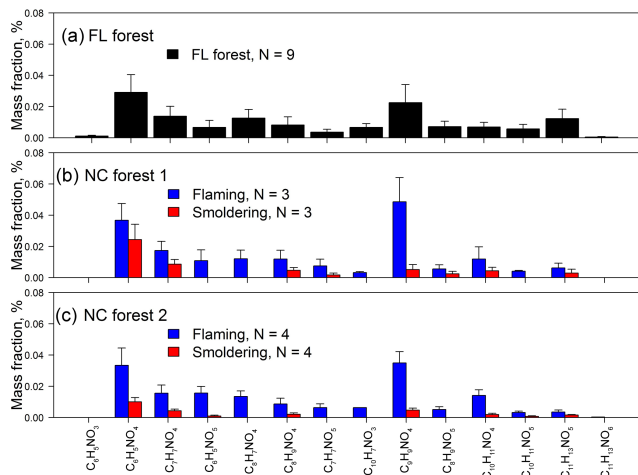


Figure 3. Relative mass contributions of identified N-containing aromatic compounds in BB samples collected during the (a) FL forest, (b) NC forest 1, and (c) NC forest 2 experiments.

ter, when domestic wood burning is prevalent (Mohr et al., 2013). In the current work, most of the NACs were quantified using surrogates, and their contributions to OM from BB may change if authentic standards or different surrogates are used for quantification. However, the three experiments might still have consistent relative mass contribution profiles of NACs and similar average tNAC_{OM} %, assuming burn conditions and fuel types have minor impact on the

OM/OC ratio. As shown in Figs. S3e and 2c, tNAC_{OM} % correlated ($p < 0.05$) with EC/OC for both individual burns and pooled experimental data. Therefore, unlike the light absorption of methanol-extractable OC, the formation of NACs in BB seems to depend largely on burn conditions rather than fuel types and ambient conditions.

Among the 14 identified NAC formulas, C₆H₅NO₄ and C₉H₉NO₄ have the highest concentrations (Fig. 3) in FL forest and NC forest flaming-phase samples, accounting for 0.029 ± 0.011 % to 0.037 ± 0.011 % and 0.023 ± 0.012 % to 0.049 ± 0.016 % of the OM, respectively (Table S3). In NC forest smoldering-phase samples, C₆H₅NO₄ has the highest mass contribution (NS1 0.024 ± 0.0098 %, NS2 0.010 ± 0.0027 %), followed by C₇H₇NO₄ (NS1 0.0087 ± 0.0030 %, NS2 0.0043 ± 0.0010 %) and C₉H₉NO₄ (NS1 0.0052 ± 0.0033 %, NS2 0.0047 ± 0.0013 %) (Table S3). The C₆H₅NO₄ was identified as 4-nitrocatechol by comparing its MS/MS spectrum (Fig. 1b) with that of an authentic standard (Fig. S2b) in Xie et al. (2017a). The EIC of C₉H₉NO₄ exhibited three to four isomers (Fig. S1i), while only two MS/MS spectra (Fig. 1l, m) were obtained due to the weak EIC intensity for compounds eluting at times ≥ 10 min. The fragmentation patterns of C₉H₉NO₄ compounds (Fig. 1l, m) are different from that of 2,5-dimethyl-4-nitrobenzoic acid (reference standards with the same formula, Fig. S2g) without the loss of CO₂, suggesting that the C₉H₉NO₄ compounds identified in this work lack a carboxylic acid group. Both MS/MS spectra of the two C₉H₉NO₄ isomers reflect the loss of OCN (Fig. 1l, m), suggesting a skeleton of benzoxazole or ben-

zisoazole or the existence of a cyanate ($-\text{O}-\text{C}\equiv\text{N}$) or isocyanate ($-\text{N}=\text{C}=\text{O}$) group. Volatile organo-isocyanate structures (e.g., CH_3NCO) were identified from anthropogenic biomass burning (Priestley et al., 2018), and benzoxazole structures have been observed in pyrolyzed charcoal smoke (Kaal et al., 2009). Giorgi et al. (2004) investigated the fragmentation of 3-methyl-1,2-benzisoxazole and 2-methyl-1,3-benzoxazole using a CID technique under different energy frames and found a loss of CO but not OCN for both of them. In this work, four standard compounds, including phenyl cyanate ($\text{C}_6\text{H}_5\text{OCN}$), benzoxazole ($\text{C}_7\text{H}_5\text{NO}$), 4-methoxyphenyl isocyanate ($\text{CH}_3\text{OC}_6\text{H}_4\text{NCO}$), and 2,4-dimethoxyphenyl isocyanate ($(\text{CH}_3\text{O})_2\text{C}_6\text{H}_3\text{NCO}$) were analyzed using a gas chromatographer (Agilent 6890) coupled to a mass spectrometer (Agilent 5975B) under electron ionization (EI, 70 eV) mode. These compounds do not have a phenol structure and cannot be detected using ESI under negative ion mode. The MS/MS spectra of 4-methoxyphenyl isocyanate and 2,4-dimethoxyphenyl isocyanate were obtained by using a modified method (ESI at positive ion mode) for NAC analysis in this work. As shown in Fig. S4a and b, the loss of OCN is observed for phenyl cyanate but not benzoxazole. In Fig. S4c and d, the ions at m/z 106 and 136 can be produced from the species at m/z 149 and 179 through the loss of $\text{CH}_3 + \text{CO}$ or $\text{H} + \text{NCO}$ (43 Da). The MS/MS spectra of 4-methoxyphenyl isocyanate and 2,4-dimethoxyphenyl isocyanate (Fig. S4e, f) confirmed the loss of $\text{CH}_3 + \text{CO}$, and the loss of CH_3 reflected the presence of a methoxy group. As such, the $\text{C}_9\text{H}_9\text{NO}_4$ compounds identified in this work are expected to contain a phenyl cyanate structure.

$\text{C}_6\text{H}_5\text{NO}_3$ (Fig. 1a) is identified as 4-nitrophenol using an authentic standard (Fig. S2a). $\text{C}_7\text{H}_7\text{NO}_4$ has at least two isomers as shown in Fig. S1c that are identified as 4-methyl-5-nitrocatechol and 3-methyl-6-nitrocatechol according to Iinuma et al. (2010) and Xie et al. (2017a). Referring to the MS/MS spectrum of 4-nitrocatechol (Fig. S2b), the $\text{C}_6\text{H}_5\text{NO}_5$ compound should have a nitrocatechol skeleton with an extra hydroxyl group on the benzene ring. Like $\text{C}_9\text{H}_9\text{NO}_4$ (Fig. 1l, m), the loss of OCN was observed for the fragmentation of $\text{C}_8\text{H}_7\text{NO}_4$ in the MS/MS spectra (Fig. 1f, g), and a phenyl cyanate structure was proposed (Table 2). However, the fragmentation mechanism associated with the loss of single nitrogen is unknown and warrants further study. The $\text{C}_8\text{H}_9\text{NO}_4$ identified in this work should have several isomers (Fig. S1f), and two representative MS/MS spectra are provided in Fig. 1h and i. The first isomer of $\text{C}_8\text{H}_9\text{NO}_4$ has a dominant ion of m/z 137, reflecting the loss of NO and CH_3 . Comparing to the MS/MS spectrum of 4-nitrophenol (Fig. S2a), the first $\text{C}_8\text{H}_9\text{NO}_4$ isomer might contain a methyl nitrophenol skeleton with a methoxy group. The fragmentation pattern of the second isomer of $\text{C}_8\text{H}_9\text{NO}_4$ is similar to $\text{C}_7\text{H}_7\text{NO}_4$, and the molecule is postulated as ethyl nitrocatechol. $\text{C}_7\text{H}_7\text{NO}_5$ has a similar fragmentation pattern to $\text{C}_6\text{H}_5\text{NO}_4$ and $\text{C}_7\text{H}_7\text{NO}_4$ and is identified as methoxy nitrocatechol. For NC forest burns, $\text{C}_{10}\text{H}_7\text{NO}_3$ was only detected

in flaming-phase samples (Fig. 3). The MS/MS spectrum of $\text{C}_{10}\text{H}_7\text{NO}_3$ was subject to considerable noise, although the loss of NO_2 could be identified (Fig. 1k). In Fig. 1n, the ion at m/z 167 is attributed to the loss of two CH_3 from the $[\text{M}-\text{H}]^-$ ion of $\text{C}_8\text{H}_9\text{NO}_5$, and the loss of $\text{H} + \text{CO} + \text{NO}$ is a common feature shared by several nitrophenol-like compounds (Fig. 1b, c, e, i), so the $\text{C}_8\text{H}_9\text{NO}_5$ compound was identified as dimethoxynitrophenol. The MS/MS spectra of $\text{C}_{10}\text{H}_{11}\text{NO}_4$, $\text{C}_{10}\text{H}_{11}\text{NO}_5$, $\text{C}_{11}\text{H}_{13}\text{NO}_5$, and $\text{C}_{11}\text{H}_{13}\text{NO}_6$ were characterized by the loss of CH_3 and/or OCN (Fig. 1o–t), indicating the existence of methoxy and/or cyanate groups (Fig. S4). Although the exact structure of these NACs cannot be determined, their functional groups on the benzene ring were proposed in Table 2 from their fragmentation patterns.

In this work, three of the identified NACs, 4-nitrophenol, 4-nitrocatechol, and methyl nitrocatechols, were commonly observed in BB emissions or BB-impacted atmospheres (Claeys et al., 2012; Mohr et al., 2013; Budisulistiorini et al., 2017). These compounds can also be generated from the photooxidation of aromatic VOCs in the presence of NO_x (Iinuma et al., 2010; Lin et al., 2015; Xie et al., 2017a). Both BB and fossil fuel combustion can emit a mixture of aromatic precursors (e.g., benzene, toluene) for secondary NAC formation (Martins et al., 2006; Lewis et al., 2013; George et al., 2014, 2015; Gilman et al., 2015; Hatch et al., 2015). Therefore, the NACs uniquely related to BB are needed to represent BB emissions. In this work, the NAC formulas with molecular weight < 200 Da (from $\text{C}_6\text{H}_5\text{NO}_3$, 138 Da; to $\text{C}_8\text{H}_9\text{NO}_5$, 198 Da) were all identified in secondary organic aerosol (SOA) generated from chamber reactions with NO_x (Xie et al., 2017a). However, the NACs from BB emissions and SOA formations with identical formulas might have different structures. For example, the MS/MS spectra of $\text{C}_7\text{H}_7\text{NO}_5$ and $\text{C}_8\text{H}_9\text{NO}_5$ from BB in this work and aromatic VOCs and NO_x reactions in Xie et al. (2017a) had distinct fragmentation patterns (Fig. S5). In Xie et al. (2017a), the $\text{C}_8\text{H}_7\text{NO}_4$ and $\text{C}_9\text{H}_9\text{NO}_4$ generated from ethylbenzene and NO_x reactions might have fragile structures and their MS/MS spectra were not available. In this work, $\text{C}_8\text{H}_7\text{NO}_4$ and $\text{C}_9\text{H}_9\text{NO}_4$ from BB emissions are more stable and are supposed to have a phenyl cyanate structure. Among the four NAC formulas with MW > 200 Da identified in this work (Table 2), $\text{C}_{10}\text{H}_{11}\text{NO}_4$ was also observed as 5-methoxy-4-nitro-2-(prop-2-en-1-yl)phenol in SOA from reactions of methyl chavicol and NO_x (Pereira et al., 2015), which cannot be assigned to the $\text{C}_{10}\text{H}_{11}\text{NO}_4$ from BB emissions in this work. Compared to the NACs in aromatic VOCs and NO_x SOA (Iinuma et al., 2010; Lin et al., 2015; Xie et al., 2017a; Pereira et al., 2015), the structures of NACs from BB in this work were characterized by methoxy and cyanate groups. The methoxyphenol structure is a feature in polar organic compounds from BB (Schauer et al., 2001; Simpson et al., 2005; Mazzoleni et al., 2007). The cyanate group was rarely reported in gas- or particle-phase pollutants from BB, which might be a missed feature of BB NACs. Vähä-Savo et

al. (2015) found that cyanate could be formed during the thermal conversion (e.g., pyrolysis, gasification) of black liquor, which is the waste product from the kraft process when digesting pulpwood into paper pulp and composed by an aqueous solution of mixed biomass residues. According to Table 2 and Fig. 3, the NACs containing methoxy and/or cyanate groups are predominately generated during the flaming phase in the two NC forest experiments. Before using these compounds as source markers for BB NACs, additional work is warranted to understand their exact structures and lifetimes in the atmosphere. The quantification of these compounds might also be subject to high variability due to the usage of surrogates.

3.3 Contribution of NACs to Abs₃₆₅

For each sample extract, individual NAC contributions to Abs₃₆₅ (Abs_{365,NAC} %) were calculated using their mass concentrations (ng m⁻³) and the MAC₃₆₅ values of individual compound standards (MAC_{365,NAC}), as applied in Zhang et al. (2013) and Xie et al. (2017a). Here, the MAC_{365,NAC} value is OM based with a unit of m² g⁻¹. Each NAC formula was assigned to an authentic or surrogate standard compound to estimate the contribution to Abs₃₆₅ of extracted OM (Table 2). Except for the NACs with a phenyl cyanate structure, the standard compounds used for the NAC absorption calculation and mass quantification were the same (Table 2), and their UV–Vis spectra were obtained from Xie et al. (2017a) and are shown in Fig. S6a. The UV–Vis spectra of three standard compounds with cyanate or isocyanate groups are given in Fig. S6b, and none of them has absorption in the range from 350 to 550 nm. As such, the NACs with cyanate groups identified in this work were supposed to have no contribution to bulk Abs₃₆₅. Details of the method for Abs_{365,NAC} % calculation are provided in Xie et al. (2017a) and the MAC_{365,NAC} values for identified NAC formulas in this work are listed in Table S4. Since the standard compounds used in this work have no absorption at 550 nm, the identified NAC contributions to Abs₅₅₀ were expected to be 0. The average and ranges of Abs_{365,NAC} % in BB samples are listed in Table S5. For simplicity, the average Abs_{365,NAC} % values in the five groups of BB samples (FF, NF1 and 2, NS1 and 2) are stacked in Fig. 4.

In general, the average contributions of total NACs to Abs₃₆₅ (Abs_{365,tNAC} % 0.087 ± 0.024 % to 1.22 ± 0.54 %) were 3–10 times higher than their average tNAC_{OM} % (0.023 ± 0.0089 % to 0.18 ± 0.067 %) in BB samples (Tables S5 and S3), indicating that the identified NACs with contributions to Abs₃₆₅ (not including those with cyanate groups) are strong BrC chromophores. Similar to the NAC mass contributions and compositions, the samples collected during flaming periods (NF1 and NF2) had a significantly higher ($p < 0.05$) average Abs_{365,tNAC} % (NF1 1.21 ± 0.38 %, NF2 0.42 ± 0.15 %) than those collected during smoldering periods (NS1 0.72 ± 0.27 %, NS2 0.087 ± 0.024 %);

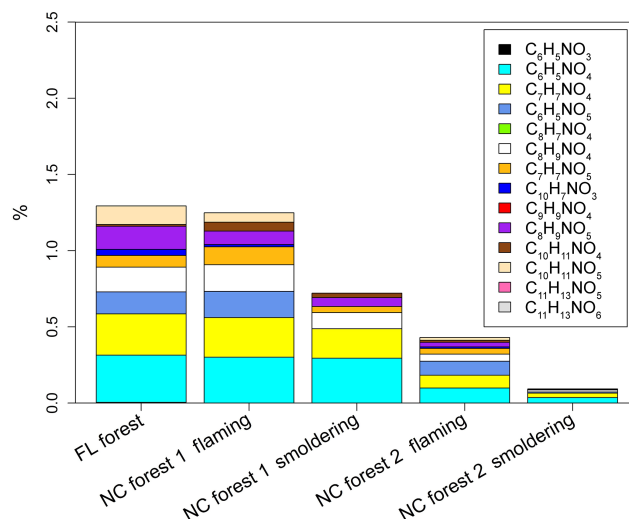


Figure 4. Average contributions (%) of N-containing aromatic compounds to Abs₃₆₅ of methanol-extractable OC from laboratory biomass burning.

Abs_{365,tNAC} % correlated ($p < 0.05$) with EC/OC for both individual burns (Fig. S3f) and pooled experimental data (Fig. 2d). C₆H₅NO₄ (0.037 ± 0.0080 % to 0.31 ± 0.11 %) and C₇H₇NO₄ (0.029 ± 0.0051 % to 0.27 ± 0.12 %) have the highest Abs_{365,NAC} % among the identified NACs across all the three BB experiments (Table S5). The average Abs_{365,tNAC} % values here are comparable to those obtained for atmospheric particles in Germany (0.10 ± 0.06 % to 1.13 ± 1.03 %) (Teich et al., 2017) and Detling, United Kingdom (4 ± 2 %) (Mohr et al., 2013), but are more than 10 times lower than those from chamber reactions of benzene (28.0 ± 8.86 %), naphthalene (20.3 ± 8.01 %), and *m*-cresol (50.5 ± 15.8 %) with NO_x (Xie et al., 2017a). Lin et al. (2016, 2017) calculated the absorbance fraction contributed by NACs in BB OC based on signal peaks at particular retention times in HPLC/PDA (photodiode array) spectrophotometry chromatograms and attributed a large portion (up to or greater than 50 %) of the solvent extract absorption to a limited number of NACs with MW mostly lower than 500 Da. However, the absorbance signals in HPLC/PDA chromatograms are composed by a mixture of light-absorbing compounds due to coelution, and some of them are not NACs or even cannot be ionized with ESI. In this study, standards or surrogates were used to calculate the absorption for individual NAC molecules. These different approaches gave different results. Di Lorenzo et al. (2017) studied the absorbance as a function of the molecular size of organic aerosols from BB and concluded that the majority of aqueous extract absorption ($\lambda = 300$ nm) was due to compounds with MW greater than 500 Da and a carbon number greater than 20. In this work, less than 2 % of the BrC absorption in BB aerosols at $\lambda = 365$ was ascribed to the identified NACs with a MW range of 138 to 254 Da, of which the contribution at a longer wavelength ($\lambda = 550$ nm)

was expected to be 0. Future work is needed to identify high-MW light-absorbing compounds in BB aerosols to apportion a greater fraction of BrC absorption in BB aerosols.

4 Conclusions

The comparisons of light-absorbing properties (MAC_{365} , MAC_{550} , and \dot{A}_{abs}) of BB OC with EC/OC in this study show that burn conditions are not the only factor impacting BrC absorption. Other factors like fuel type or ambient conditions may also play important roles in determining BrC absorption from BB. It may be impractical to predict BrC absorption solely based on EC/OC ratios in BB emissions from different fuels or over different seasons. The present study identified 14 NAC chemical formulas in BB aerosols. The average $tNAC_{OM}$ % values of the FL forest, NC forest 1, and NC forest 2 (flaming and smoldering samples were combined) experiments were 0.13 ± 0.059 %, 0.13 ± 0.067 %, and 0.11 ± 0.017 % by weight, respectively, and the NAC composition was also similar across the three BB experiments. Most of the NAC formulas identified in this work were also observed in simulated SOA generated from chamber reactions of aromatic VOCs with NO_x , but the same NAC formula from BB and SOA could not be assigned to the identical compound. In this work, the structures of NACs from BB were characterized by methoxy and cyanate groups, which were predominately generated during the flaming phase and might be an important feature for BB NACs. More work is warranted to understand their exact structures and lifetimes. The average $tNAC_{OM}$ % and $Abs_{365,tNAC}$ % of the flaming-phase samples were significantly higher ($p < 0.05$) than those of smoldering-phase samples in the two NC forest BB experiments. Unlike the bulk MAC_{365} and MAC_{550} , $tNAC_{OM}$ % and $Abs_{365,tNAC}$ % correlated ($p < 0.05$) with EC/OC for both individual burns and pooled experimental data, suggesting that burn conditions are an important factor in determining NAC formation in BB. Except for the compounds with cyanate groups, the NACs identified in this work are likely strong BrC chromophores, as the average contributions of total NACs to bulk Abs_{365} ($0.0.087 \pm 0.024$ % to 1.22 ± 0.54 %) are 3–10 times higher than their average mass contributions to OM (0.023 ± 0.0089 % to 0.18 ± 0.067 %). However, more light-absorbing compounds from BB with high MW need to be identified to apportion the unknown fraction (> 98 %) of BrC absorption.

Data availability. Data used in the writing of this paper are available at the U.S. Environmental Protection Agency's Environmental Dataset Gateway (<https://edg.epa.gov>, last access: 4 March 2019).

Supplement. The supplement related to this article is available online at: <https://doi.org/10.5194/acp-19-2899-2019-supplement>.

Author contributions. MX and ALH designed the research. MX and XC performed the experiments. ALH and MDH managed sample collection. MX analyzed the data and wrote the paper with significant contributions from all co-authors.

Competing interests. The authors declare that they have no conflict of interest.

Disclaimer. The views expressed in this article are those of the authors and do not necessarily represent the views or policies of the U.S. Environmental Protection Agency.

Acknowledgements. This research was supported by the National Natural Science Foundation of China (NSFC, 41701551), the State Key Laboratory of Pollution Control and Resource Reuse Foundation (no. PCRRF17040), and the Startup Foundation for Introducing Talent of NUIST (no. 2243141801001). We would like to acknowledge Brian Gullett, Johanna Aurell, and Brannon Seay for assistance with laboratory biomass burning sampling. This work was funded by the U.S. Environmental Protection Agency.

Edited by: Yinon Rudich

Reviewed by: three anonymous referees

References

- Akagi, S. K., Yokelson, R. J., Wiedinmyer, C., Alvarado, M. J., Reid, J. S., Karl, T., Crounse, J. D., and Wennberg, P. O.: Emission factors for open and domestic biomass burning for use in atmospheric models, *Atmos. Chem. Phys.*, 11, 4039–4072, <https://doi.org/10.5194/acp-11-4039-2011>, 2011.
- Anderson, T. L., Charlson, R. J., Schwartz, S. E., Knutti, R., Boucher, O., Rodhe, H., and Heintzenberg, J.: Climate forcing by aerosols—a hazy picture, *Science*, 300, 1103–1104, <https://doi.org/10.1126/science.1084777>, 2003.
- Aurell, J. and Gullett, B. K.: Emission factors from aerial and ground measurements of field and laboratory forest burns in the southeastern U.S.: $PM_{2.5}$, black and brown carbon, VOC, and PCDD/PCDF, *Environ. Sci. Technol.*, 47, 8443–8452, <https://doi.org/10.1021/es402101k>, 2013.
- Aurell, J., Gullett, B. K., and Tabor, D.: Emissions from southeastern U.S. grasslands and pine savannas: comparison of aerial and ground field measurements with laboratory burns, *Atmos. Environ.*, 111, 170–178, <https://doi.org/10.1016/j.atmosenv.2015.03.001>, 2015.
- Bond, T. C.: Spectral dependence of visible light absorption by carbonaceous particles emitted from coal combustion, *Geophys. Res. Lett.*, 28, 4075–4078, <https://doi.org/10.1029/2001gl013652>, 2001.
- Bond, T. C. and Bergstrom, R. W.: Light absorption by carbonaceous particles: an investigative review, *Aerosol Sci. Technol.*, 40, 27–67, <https://doi.org/10.1080/02786820500421521>, 2006.
- Bond, T. C., Streets, D. G., Yarber, K. F., Nelson, S. M., Woo, J.-H., and Klimont, Z.: A technology-based global inventory of black

- and organic carbon emissions from combustion, *J. Geophys. Res.*, 109, D14, <https://doi.org/10.1029/2003jd003697>, 2004.
- Bond, T. C., Doherty, S. J., Fahey, D. W., Forster, P. M., Berntsen, T., DeAngelo, B. J., Flanner, M. G., Ghan, S., Kärcher, B., Koch, D., Kinne, S., Kondo, Y., Quinn, P. K., Sarofim, M. C., Schultz, M. G., Schulz, M., Venkataraman, C., Zhang, H., Zhang, S., Bellouin, N., Guttikunda, S. K., Hopke, P. K., Jacobson, M. Z., Kaiser, J. W., Klimont, Z., Lohmann, U., Schwarz, J. P., Shindell, D., Storelvmo, T., Warren, S. G., and Zender, C. S.: Bounding the role of black carbon in the climate system: A scientific assessment, *J. Geophys. Res.*, 118, 5380–5552, <https://doi.org/10.1002/jgrd.50171>, 2013.
- Budisulistiorini, S. H., Riva, M., Williams, M., Chen, J., Itoh, M., Surratt, J. D., and Kuwata, M.: Light-absorbing brown carbon aerosol constituents from combustion of Indonesian peat and biomass, *Environ. Sci. Technol.*, 51, 4415–4423, <https://doi.org/10.1021/acs.est.7b00397>, 2017.
- Chakrabarty, R. K., Moosmüller, H., Chen, L.-W. A., Lewis, K., Arnott, W. P., Mazzoleni, C., Dubey, M. K., Wold, C. E., Hao, W. M., and Kreidenweis, S. M.: Brown carbon in tar balls from smoldering biomass combustion, *Atmos. Chem. Phys.*, 10, 6363–6370, <https://doi.org/10.5194/acp-10-6363-2010>, 2010.
- Chakrabarty, R. K., Gyawali, M., Yatavelli, R. L. N., Pandey, A., Watts, A. C., Knue, J., Chen, L.-W. A., Pattison, R. R., Tsbart, A., Samburova, V., and Moosmüller, H.: Brown carbon aerosols from burning of boreal peatlands: microphysical properties, emission factors, and implications for direct radiative forcing, *Atmos. Chem. Phys.*, 16, 3033–3040, <https://doi.org/10.5194/acp-16-3033-2016>, 2016.
- Chen, L. W. A., Doddridge, B. G., Dickerson, R. R., Chow, J. C., Mueller, P. K., Quinn, J., and Butler, W. A.: Seasonal variations in elemental carbon aerosol, carbon monoxide and sulfur dioxide: Implications for sources, *Geophys. Res. Lett.*, 28, 1711–1714, <https://doi.org/10.1029/2000gl012354>, 2001.
- Chen, Y. and Bond, T. C.: Light absorption by organic carbon from wood combustion, *Atmos. Chem. Phys.*, 10, 1773–1787, <https://doi.org/10.5194/acp-10-1773-2010>, 2010.
- Chen, Y., Sheng, G., Bi, X., Feng, Y., Mai, B., and Fu, J.: Emission factors for carbonaceous particles and polycyclic aromatic hydrocarbons from residential coal combustion in China, *Environ. Sci. Technol.*, 39, 1861–1867, <https://doi.org/10.1021/es0493650>, 2005.
- Chow, K. S., Huang, X. H. H., and Yu, J. Z.: Quantification of nitroaromatic compounds in atmospheric fine particulate matter in Hong Kong over 3 years: field measurement evidence for secondary formation derived from biomass burning emissions, *Environ. Chem.*, 13, 665–673, <https://doi.org/10.1071/EN15174>, 2016.
- Chung, S. H. and Seinfeld, J. H.: Global distribution and climate forcing of carbonaceous aerosols, *J. Geophys. Res.*, 107, AAC 14-11–AAC 14-33, <https://doi.org/10.1029/2001jd001397>, 2002.
- Claeys, M., Vermeylen, R., Yasmeeen, F., Gómez-González, Y., Chi, X., Maenhaut, W., Mészáros, T., and Salma, I.: Chemical characterisation of humic-like substances from urban, rural and tropical biomass burning environments using liquid chromatography with UV/vis photodiode array detection and electrospray ionisation mass spectrometry, *Environ. Chem.*, 9, 273–284, <https://doi.org/10.1071/EN11163>, 2012.
- Desyaterik, Y., Sun, Y., Shen, X., Lee, T., Wang, X., Wang, T., and Collett, J. L.: Speciation of “brown” carbon in cloud water impacted by agricultural biomass burning in eastern China, *J. Geophys. Res.*, 118, 7389–7399, <https://doi.org/10.1002/jgrd.50561>, 2013.
- Di Lorenzo, R. A., Washenfelder, R. A., Attwood, A. R., Guo, H., Xu, L., Ng, N. L., Weber, R. J., Baumann, K., Edgerton, E., and Young, C. J.: Molecular-size-separated brown carbon absorption for biomass-burning aerosol at multiple field sites, *Environ. Sci. Technol.*, 51, 3128–3137, <https://doi.org/10.1021/acs.est.6b06160>, 2017.
- Eriksson, A., Nordin, E., Nystrom, R., Pettersson, E., Swietlicki, E., Bergvall, C., Westerholm, R., Boman, C., and Pagels, J.: Particulate PAH emissions from residential biomass combustion: time-resolved analysis with aerosol mass spectrometry, *Environ. Sci. Technol.*, 48, 7143–7150, <https://doi.org/10.1021/es500486j>, 2014.
- George, I. J., Hays, M. D., Snow, R., Faircloth, J., George, B. J., Long, T., and Baldauf, R. W.: Cold temperature and biodiesel fuel effects on speciated emissions of volatile organic compounds from diesel trucks, *Environ. Sci. Technol.*, 48, 14782–14789, <https://doi.org/10.1021/es502949a>, 2014.
- George, I. J., Hays, M. D., Herrington, J. S., Preston, W., Snow, R., Faircloth, J., George, B. J., Long, T., and Baldauf, R. W.: Effects of cold temperature and ethanol content on VOC emissions from light-duty gasoline vehicles, *Environ. Sci. Technol.*, 49, 13067–13074, <https://doi.org/10.1021/acs.est.5b04102>, 2015.
- Gilman, J. B., Lerner, B. M., Kuster, W. C., Goldan, P. D., Warneke, C., Veres, P. R., Roberts, J. M., de Gouw, J. A., Burling, I. R., and Yokelson, R. J.: Biomass burning emissions and potential air quality impacts of volatile organic compounds and other trace gases from fuels common in the US, *Atmos. Chem. Phys.*, 15, 13915–13938, <https://doi.org/10.5194/acp-15-13915-2015>, 2015.
- Giorgi, G., Salvini, L., and Ponticelli, F.: Gas phase ion chemistry of the heterocyclic isomers 3-methyl-1,2-benzisoxazole and 2-methyl-1,3-benzoxazole, *J. Am. Soc. Mass Spectrom.*, 15, 1005–1013, <https://doi.org/10.1016/j.jasms.2004.04.002>, 2004.
- Grandesso, E., Gullett, B., Touati, A., and Tabor, D.: Effect of moisture, charge size, and chlorine concentration on PCDD/F emissions from simulated open burning of forest biomass, *Environ. Sci. Technol.*, 45, 3887–3894, <https://doi.org/10.1021/es103686t>, 2011.
- Hatch, L. E., Luo, W., Pankow, J. F., Yokelson, R. J., Stockwell, C. E., and Barsanti, K. C.: Identification and quantification of gaseous organic compounds emitted from biomass burning using two-dimensional gas chromatography–time-of-flight mass spectrometry, *Atmos. Chem. Phys.*, 15, 1865–1899, <https://doi.org/10.5194/acp-15-1865-2015>, 2015.
- Hecobian, A., Zhang, X., Zheng, M., Frank, N., Edgerton, E. S., and Weber, R. J.: Water-Soluble Organic Aerosol material and the light-absorption characteristics of aqueous extracts measured over the Southeastern United States, *Atmos. Chem. Phys.*, 10, 5965–5977, <https://doi.org/10.5194/acp-10-5965-2010>, 2010.
- Holder, A. L., Hagler, G. S. W., Aurell, J., Hays, M. D., and Gullett, B. K.: Particulate matter and black carbon optical properties and emission factors from prescribed fires in the southeastern United States, *J. Geophys. Res.*, 121, 3465–3483, <https://doi.org/10.1002/2015jd024321>, 2016.

- Hosseini, S., Urbanski, S., Dixit, P., Qi, L., Burling, I. R., Yokelson, R. J., Johnson, T. J., Shrivastava, M., Jung, H., and Weise, D. R.: Laboratory characterization of PM emissions from combustion of wildland biomass fuels, *J. Geophys. Res.*, 118, 9914–9929, <https://doi.org/10.1002/jgrd.50481>, 2013.
- Huang, R.-J., Yang, L., Cao, J., Chen, Y., Chen, Q., Li, Y., Duan, J., Zhu, C., Dai, W., Wang, K., Lin, C., Ni, H., Corbin, J. C., Wu, Y., Zhang, R., Tie, X., Hoffmann, T., O'Dowd, C., and Dusek, U.: Brown carbon aerosol in urban Xi'an, Northwest China: the composition and light absorption properties, *Environ. Sci. Technol.*, 52, 6825–6833, <https://doi.org/10.1021/acs.est.8b02386>, 2018.
- Iinuma, Y., Böge, O., Gräfe, R., and Herrmann, H.: Methyl-nitrocatechols: atmospheric tracer compounds for biomass burning secondary organic aerosols, *Environ. Sci. Technol.*, 44, 8453–8459, <https://doi.org/10.1021/es102938a>, 2010.
- Kaal, J., Martínez Cortizas, A., and Nierop, K. G. J.: Characterisation of aged charcoal using a coil probe pyrolysis-GC/MS method optimised for black carbon, *J. Anal. Appl. Pyrol.*, 85, 408–416, <https://doi.org/10.1016/j.jaap.2008.11.007>, 2009.
- Kirchstetter, T. W., Novakov, T., and Hobbs, P. V.: Evidence that the spectral dependence of light absorption by aerosols is affected by organic carbon, *J. Geophys. Res.*, 109, D21208, <https://doi.org/10.1029/2004jd004999>, 2004.
- Lack, D. A. and Langridge, J. M.: On the attribution of black and brown carbon light absorption using the Ångström exponent, *Atmos. Chem. Phys.*, 13, 10535–10543, <https://doi.org/10.5194/acp-13-10535-2013>, 2013.
- Laskin, A., Laskin, J., and Nizkorodov, S. A.: Chemistry of atmospheric brown carbon, *Chem. Rev.*, 115, 4335–4382, <https://doi.org/10.1021/cr5006167>, 2015.
- Lewis, A. C., Evans, M. J., Hopkins, J. R., Punjabi, S., Read, K. A., Purvis, R. M., Andrews, S. J., Moller, S. J., Carpenter, L. J., Lee, J. D., Rickard, A. R., Palmer, P. I., and Parrington, M.: The influence of biomass burning on the global distribution of selected non-methane organic compounds, *Atmos. Chem. Phys.*, 13, 851–867, <https://doi.org/10.5194/acp-13-851-2013>, 2013.
- Lin, P., Liu, J. M., Shilling, J. E., Kathmann, S. M., Laskin, J., and Laskin, A.: Molecular characterization of brown carbon (BrC) chromophores in secondary organic aerosol generated from photo-oxidation of toluene, *Phys. Chem. Chem. Phys.*, 17, 23312–23325, <https://doi.org/10.1039/c5cp02563j>, 2015.
- Lin, P., Aiona, P. K., Li, Y., Shiraiwa, M., Laskin, J., Nizkorodov, S. A., and Laskin, A.: Molecular characterization of brown carbon in biomass burning aerosol particles, *Environ. Sci. Technol.*, 50, 11815–11824, <https://doi.org/10.1021/acs.est.6b03024>, 2016.
- Lin, P., Bluvshstein, N., Rudich, Y., Nizkorodov, S. A., Laskin, J., and Laskin, A.: Molecular chemistry of atmospheric brown carbon inferred from a nationwide biomass burning event, *Environ. Sci. Technol.*, 51, 11561–11570, <https://doi.org/10.1021/acs.est.7b02276>, 2017.
- Lin, Y.-H., Budisulistiorini, S. H., Chu, K., Siejack, R. A., Zhang, H., Riva, M., Zhang, Z., Gold, A., Kautzman, K. E., and Surratt, J. D.: Light-absorbing oligomer formation in secondary organic aerosol from reactive uptake of isoprene epoxydiols, *Environ. Sci. Technol.*, 48, 12012–12021, <https://doi.org/10.1021/es503142b>, 2014.
- Lu, Z., Streets, D. G., Winijkul, E., Yan, F., Chen, Y., Bond, T. C., Feng, Y., Dubey, M. K., Liu, S., Pinto, J. P., and Carmichael, G. R.: Light absorption properties and radiative effects of primary organic aerosol emissions, *Environ. Sci. Technol.*, 49, 4868–4877, <https://doi.org/10.1021/acs.est.5b00211>, 2015.
- Martins, L. D., Andrade, M. F., Freitas, E. D., Preto, A., Gatti, L. V., Albuquerque, É. L., Tomaz, E., Guardani, M. L., Martins, M. H. R. B., and Junior, O. M. A.: Emission factors for gas-powered vehicles traveling through road tunnels in São Paulo, Brazil, *Environ. Sci. Technol.*, 40, 6722–6729, <https://doi.org/10.1021/es052441u>, 2006.
- Martinsson, J., Eriksson, A., Nielsen, I. E., Malmberg, V. B., Ahlberg, E., Andersen, C., Lindgren, R., Nystrom, R., Nordin, E., and Brune, W.: Impacts of combustion conditions and photochemical processing on the light absorption of biomass combustion aerosol, *Environ. Sci. Technol.*, 49, 14663–14671, <https://doi.org/10.1021/acs.est.5b03205>, 2015.
- Mazzoleni, L. R., Zielinska, B., and Moosmüller, H.: Emissions of levoglucosan, methoxy phenols, and organic acids from prescribed burns, laboratory combustion of wildland fuels, and residential wood combustion, *Environ. Sci. Technol.*, 41, 2115–2122, <https://doi.org/10.1021/es061702c>, 2007.
- McMeeking, G., Fortner, E., Onasch, T., Taylor, J., Flynn, M., Coe, H., and Kreidenweis, S.: Impacts of nonrefractory material on light absorption by aerosols emitted from biomass burning, *J. Geophys. Res.*, 119, 12272–12286, 2014.
- Mohr, C., Lopez-Hilfiker, F. D., Zotter, P., Prévôt, A. S. H., Xu, L., Ng, N. L., Herndon, S. C., Williams, L. R., Franklin, J. P., Zahniser, M. S., Worsnop, D. R., Knighton, W. B., Aiken, A. C., Gorkowski, K. J., Dubey, M. K., Allan, J. D., and Thornton, J. A.: Contribution of nitrated phenols to wood burning brown carbon light absorption in Detling, United Kingdom during winter time, *Environ. Sci. Technol.*, 47, 6316–6324, <https://doi.org/10.1021/es400683v>, 2013.
- Myhre, G., Samset, B. H., Schulz, M., Balkanski, Y., Bauer, S., Bernsten, T. K., Bian, H., Bellouin, N., Chin, M., Diehl, T., Easter, R. C., Feichter, J., Ghan, S. J., Hauglustaine, D., Iversen, T., Kinne, S., Kirkevåg, A., Lamarque, J.-F., Lin, G., Liu, X., Lund, M. T., Luo, G., Ma, X., van Noije, T., Penner, J. E., Rasch, P. J., Ruiz, A., Seland, Ø., Skeie, R. B., Stier, P., Takemura, T., Tsigaridis, K., Wang, P., Wang, Z., Xu, L., Yu, H., Yu, F., Yoon, J.-H., Zhang, K., Zhang, H., and Zhou, C.: Radiative forcing of the direct aerosol effect from AeroCom Phase II simulations, *Atmos. Chem. Phys.*, 13, 1853–1877, <https://doi.org/10.5194/acp-13-1853-2013>, 2013.
- Nielsen, I. E., Eriksson, A. C., Lindgren, R., Martinsson, J., Nystrom, R., Nordin, E. Z., Sadiktsis, I., Boman, C., Nøjgaard, J. K., and Pagels, J.: Time-resolved analysis of particle emissions from residential biomass combustion – Emissions of refractory black carbon, PAHs and organic tracers, *Atmos. Environ.*, 165, 179–190, 2017.
- NIOSH: National Institute of Occupational Safety and Health, Elemental carbon (diesel particulate), Method 5040, available at: <https://www.cdc.gov/niosh/docs/2003-154/pdfs/5040f3.pdf> (last access: March 2018), 1999.
- Pereira, K. L., Hamilton, J. F., Rickard, A. R., Bloss, W. J., Alam, M. S., Camredon, M., Ward, M. W., Wyche, K. P., Muñoz, A., Vera, T., Vázquez, M., Borrás, E., and Ródenas, M.: Insights into the formation and evolution of individual compounds in the particulate phase during aromatic photo-oxidation, *Environ. Sci. Technol.*, 49, 13168–13178, <https://doi.org/10.1021/acs.est.5b03377>, 2015.

- Pokhrel, R. P., Wagner, N. L., Langridge, J. M., Lack, D. A., Jayarathne, T., Stone, E. A., Stockwell, C. E., Yokelson, R. J., and Murphy, S. M.: Parameterization of single-scattering albedo (SSA) and absorption Ångström exponent (AAE) with EC/OC for aerosol emissions from biomass burning, *Atmos. Chem. Phys.*, 16, 9549–9561, <https://doi.org/10.5194/acp-16-9549-2016>, 2016.
- Priestley, M., Le Breton, M., Bannan, T. J., Leather, K. E., Bacak, A., Reyes-Villegas, E., De Vocht, F., Shallcross, B. M. A., Brazier, T., Anwar Khan, M., Allan, J., Shallcross, D. E., Coe, H., and Percival, C. J.: Observations of isocyanate, amide, nitrate, and nitro compounds from an anthropogenic biomass burning event using a ToF-CIMS, *J. Geophys. Res.*, 123, 7687–7704, <https://doi.org/10.1002/2017JD027316>, 2018.
- Ramanathan, V., Crutzen, P. J., Kiehl, J. T., and Rosenfeld, D.: Aerosols, climate, and the hydrological cycle, *Science*, 294, 2119–2124, <https://doi.org/10.1126/science.1064034>, 2001.
- Reff, A., Bhave, P. V., Simon, H., Pace, T. G., Pouliot, G. A., Mobley, J. D., and Houyoux, M.: Emissions inventory of PM_{2.5} trace elements across the United States, *Environ. Sci. Technol.*, 43, 5790–5796, <https://doi.org/10.1021/es802930x>, 2009.
- Riddle, S. G., Jakober, C. A., Robert, M. A., Cahill, T. M., Charles, M. J., and Kleeman, M. J.: Large PAHs detected in fine particulate matter emitted from light-duty gasoline vehicles, *Atmos. Environ.*, 41, 8658–8668, <https://doi.org/10.1016/j.atmosenv.2007.07.023>, 2007.
- Saleh, R., Robinson, E. S., Tkacik, D. S., Ahern, A. T., Liu, S., Aiken, A. C., Sullivan, R. C., Presto, A. A., Dubey, M. K., Yokelson, R. J., Donahue, N. M., and Robinson, A. L.: Brownness of organics in aerosols from biomass burning linked to their black carbon content, *Nature Geosci.*, 7, 647–650, <https://doi.org/10.1038/ngeo2220>, 2014.
- Samburova, V., Connolly, J., Gyawali, M., Yatavelli, R. L. N., Watts, A. C., Chakrabarty, R. K., Zielinska, B., Moosmüller, H., and Khlystov, A.: Polycyclic aromatic hydrocarbons in biomass-burning emissions and their contribution to light absorption and aerosol toxicity, *Sci. Total Environ.*, 568, 391–401, <https://doi.org/10.1016/j.scitotenv.2016.06.026>, 2016.
- Schauer, J. J., Kleeman, M. J., Cass, G. R., and Simoneit, B. R. T.: Measurement of emissions from air pollution sources. 3. C₁–C₂₉ organic compounds from fireplace combustion of wood, *Environ. Sci. Technol.*, 35, 1716–1728, <https://doi.org/10.1021/es001331e>, 2001.
- Simpson, C. D., Paulsen, M., Dills, R. L., Liu, L. J. S., and Kalman, D. A.: Determination of methoxyphenols in ambient atmospheric particulate matter: tracers for wood combustion, *Environ. Sci. Technol.*, 39, 631–637, <https://doi.org/10.1021/es0486871>, 2005.
- Teich, M., van Pinxteren, D., Kecorius, S., Wang, Z., and Herrmann, H.: First quantification of imidazoles in ambient aerosol particles: potential photosensitizers, brown carbon constituents, and hazardous components, *Environ. Sci. Technol.*, 50, 1166–1173, <https://doi.org/10.1021/acs.est.5b05474>, 2016.
- Teich, M., van Pinxteren, D., Wang, M., Kecorius, S., Wang, Z., Müller, T., Mocnik, G., and Herrmann, H.: Contributions of nitrated aromatic compounds to the light absorption of water-soluble and particulate brown carbon in different atmospheric environments in Germany and China, *Atmos. Chem. Phys.*, 17, 1653–1672, <https://doi.org/10.5194/acp-17-1653-2017>, 2017.
- Vähä-Savo, N., DeMartini, N., Engblom, M., Brink, A., and Hupa, M.: The fate of char nitrogen in black liquor combustion – Cyanate formation and decomposition, *Ind. Eng. Chem. Res.*, 54, 2831–2842, <https://doi.org/10.1021/ie503450r>, 2015.
- Xie, M., Chen, X., Hays, M. D., Lewandowski, M., Offenberg, J., Kleindienst, T. E., and Holder, A. L.: Light absorption of secondary organic aerosol: composition and contribution of nitroaromatic compounds, *Environ. Sci. Technol.*, 51, 11607–11616, <https://doi.org/10.1021/acs.est.7b03263>, 2017a.
- Xie, M., Hays, M. D., and Holder, A. L.: Light-absorbing organic carbon from prescribed and laboratory biomass burning and gasoline vehicle emissions, *Sci. Rep.-UK*, 7, 7318, <https://doi.org/10.1038/s41598-017-06981-8>, 2017b.
- Zhang, X., Lin, Y.-H., Surratt, J. D., and Weber, R. J.: Sources, composition and absorption Ångström exponent of light-absorbing organic components in aerosol extracts from the Los Angeles Basin, *Environ. Sci. Technol.*, 47, 3685–3693, <https://doi.org/10.1021/es305047b>, 2013.
- Zhou, Y., Xing, X., Lang, J., Chen, D., Cheng, S., Wei, L., Wei, X., and Liu, C.: A comprehensive biomass burning emission inventory with high spatial and temporal resolution in China, *Atmos. Chem. Phys.*, 17, 2839–2864, <https://doi.org/10.5194/acp-17-2839-2017>, 2017.